2001

The cloud, aerosol and precipitation spectrometer: a new instrument for cloud investigations

Baumgardner, D.; Jonsson, H.; Dawson, W.; O'Connor, D.; Newton, R.

Atmospheric Research 5960 (2001) 251 264
http://hdl.handle.net/10945/46132

ELSEVIER

Atmospheric Research 59–60 (2001) 251–264

ATMOSPHERIC RESEARCH

www.elsevier.com/locate/atmos

The cloud, aerosol and precipitation spectrometer: a new instrument for cloud investigations

D. Baumgardner [a,b,*], H. Jonsson [c], W. Dawson [a], D. O'Connor [a], R. Newton [a]

[a] *Droplet Measurement Technologies, Boulder, CO 80308, USA*
[b] *Universidad Nacional Autónoma de México, Mexico City, Mexico*
[c] *Naval Post Graduate School, Monterey, CA, USA*

Accepted 27 July 2001

Abstract

A new airborne particle spectrometer has been developed with the same measurement capabilities of the Forward Scattering Spectrometer Probes (FSSP) models 100 and 300 (FSSP-300 and FSSP-100), two-dimensional optical imaging probe (2D-OAP), the Multiangle Aerosol Spectrometer Probe (MASP) and hot-wire liquid water probe, but with a single integrated system. The cloud, aerosol and precipitation spectrometer (CAPS) measures particles from 0.35 μm to 1.55 mm in diameter and liquid water content (LWC) from 0.01 to 3 g m^{-3}. In addition to combining five probes into one, it measures airspeed at the sample volume and transmits a data stream that requires no special interfaces to communicate with most computers.

Keywords: Particle measurements; Aerosol spectrometer; Cloud droplet spectrometer

1. Introduction

The PMS[1] Forward Scattering Spectrometer Probe (FSSP) models 100 and 300 (FSSP-100 and -300) and two-dimensional optical imaging probes (2D-OAP) are the most commonly used instruments currently in use for airborne measurements of size and concentration of atmospheric aerosol and cloud particles larger than 0.3 μm. The hot-wire

* Corresponding author. Universidad Nacional Autónoma de México, Mexico City, Mexico. Fax: +52-5-622-4248.

E-mail address: darrel@servidor.unam.mx (D. Baumgardner).

[1] Particle Measuring Systems, Boulder, CO. Note that these instruments are now built and marketed by Particle Metrics (PMI), Boulder.

0169-8095/01/$ - see front matter
PII: S0169-8095(01)00119-3

probe (King et al., 1978) is most widely used for liquid water content (LWC) measurements. More recently, the Multiangle Aerosol Spectrometer Probe (MASP) has been used to measure aerosol size distributions and estimate the particle composition (Baumgardner et al., 1996), particularly in the stratosphere and upper troposphere. The aforementioned measurement techniques are well characterized, and extensive research on the uncertainties has established the principal operating limitations for these measurement techniques (e.g., Knollenberg, 1981; Baumgardner, 1983; Baumgardner et al., 1985, 1990, 1992; Baumgardner and Spowart, 1990; Baumgardner and Korolev, 1997; Brenguier and Amodei, 1989a,b; Brenguier et al., 1994, 1998; Dye and Baumgardner, 1984; Korolev et al., 1991, 1998; Wendisch et al., 1996).

The primary uncertainty in concentration measurements with the light scattering instruments, i.e. FSSP-100 and FSSP-300, is associated with counting losses related to electronic dead time and coincidence (Baumgardner et al., 1985; Brenguier and Amodei, 1989a,b; Brenguier et al., 1994). There are sizing uncertainties caused by electronic roll-off and laser beam inhomogeneity (Baumgardner and Spowart, 1990; Wendisch et al., 1996). In addition, these instruments have a limited number of channels with fixed size thresholds that limit the amount of information that can be obtained about the shape of the size distribution (Brenguier et al., 1998).

Primary limitations of the 2D probe are the uncertainties in sizing related to optical diffraction (Korolev et al., 1991, 1998) and sample volume definition related to the electronic response time (Baumgardner and Korolev, 1997). An additional limitation is associated with the sampling rate of these probes. In order to record an undistorted image, the 2D probes must sample a particle as it moves across the diode array (see Section 2) by a distance equal to the probe resolution. This sample rate is the ratio of the airspeed to the probe resolution. Current 2D probes can only sample up to a sample rate of approximately 5 MHz. This means that the size resolution is limited by the airspeed, e.g. at 100 m s^{-1}, the probe resolution can be no smaller than 20 μm. For research aircraft like the NASA DC-8 that flies at 200 m s^{-1}, the minimum size resolution is 40 μm.

Another problem with 2D probes is that the clock rate sent to them by the data system can be in error. The data system must communicate with the probe to set the clock rate based on the measured airspeed since there is no direct measurement of the airspeed on 2D probes. The airspeed used to set these sample rates is normally measured at a location different than that of the probes. This adds additional uncertainty since the air velocity at the probe location, e.g. on a wing tip, can be quite different than where the velocity is measured, e.g. at the aircraft nose. Additional problems arise due to particle losses during periods when image storage space in the probe is exceeded and the instrument must wait until the data are transferred to the data system before new images can be stored.

In order to analyze the complete aerosol, droplet and precipitation size distribution, the measurements from the three types of PMS probes must be combined to produce a single spectrum. In the majority of instances where multiple probes are deployed on a research aircraft, the probes cannot be co-located and particle samples will be taken from the volumes that may be separated by meters to tens of meters. In clouds where the microphysical properties are not homogeneous spatially or temporally, this separation in the measurement volumes complicates the interpretation of microphysical data.

The introduction in 1999 of the Droplet Measurement Technologies (DMT) cloud, aerosol and precipitation spectrometer (CAPS) addressed and minimized many of the uncertainties and limitations associated with the PMS probes by utilizing state-of-the-art optics and electronics. The CAPS, as described below, takes the functionality of the PMS FSSP-300, FSSP-100, 2D-OAP, MASP and hot-wire liquid water sensors and combines them into a single instrument.

2. Operating principles of the CAPS

The CAPS shown in Fig. 1 consists of five sensors: the cloud and aerosol spectrometer (CAS: 0.35–50 μm), the cloud imaging probe (CIP: 25–1550 μm), the liquid water content detector (LWCD: 0.01–3 g m^{-3}), an air speed sensor and a temperature probe. The geometry of the CAPS is such that it is plug-compatible with the popular PMS canister that mounts on the aircraft fuselage or wing.

The CAS measurement technique (Fig. 2) is similar to FSSP-100, i.e. collection of forward-scattered light (4–13°) from single particles passing through a focused laser beam. In contrast to the 2-mW multimode HeNe gas laser of the FSSP, a 45-mW Gaussian mode diode laser with a wavelength of 0.685 μm was used. The sample volume of the CAS is defined with a pinhole aperture similar to the slit aperture used in FSSP-300 (Baumgardner et al., 1992) and is used to select only the most intense section of the laser beam. The sample area of 0.118 mm^2 is about half of that of FSSP-100 (0.3 mm^2) and three times that of FSSP-300 (0.05 mm^2).

The CAS has an additional set of optics and detectors that measure backscattered light (5–14°). The size of each particle is determined using Mie scattering theory and by assuming spherical particles of known refractive index. The size is determined from both forward- and backward-scattered light, and a comparison of the sizes derived from the two

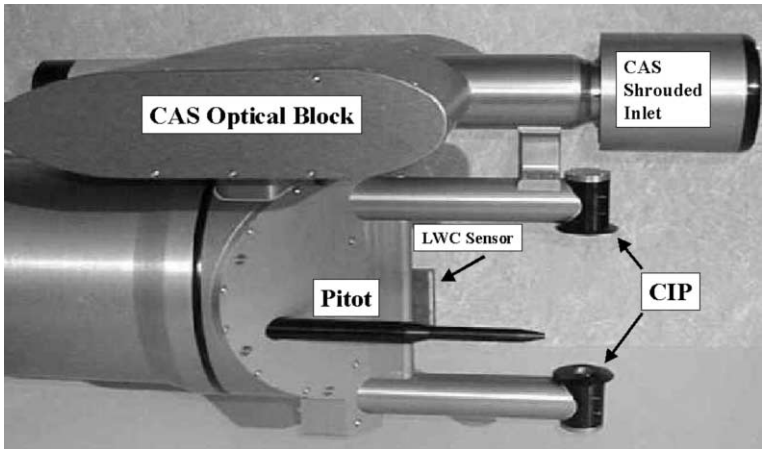

Fig. 1. The CAPS can be installed in a standard PMS canister for mounting on an aircraft as shown in this photograph. The different sensor types are annotated in the text boxes and described in the text.

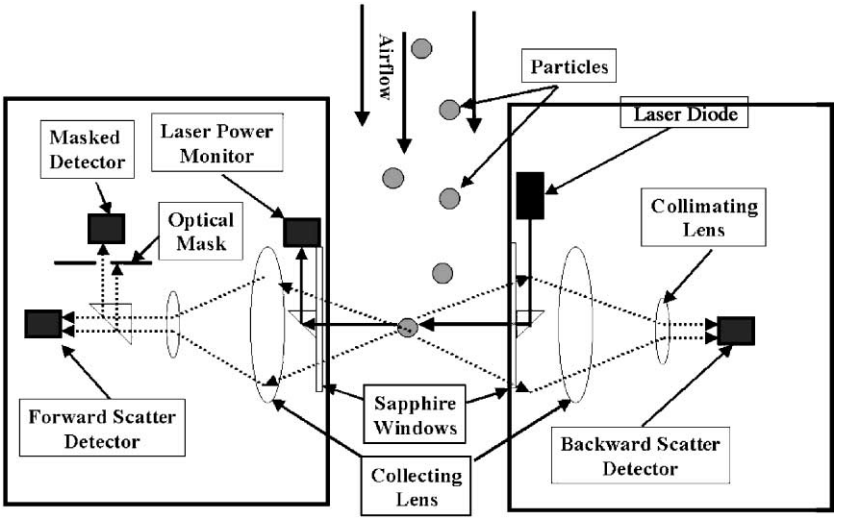

Fig. 2. The optical light collection configuration for CAS is shown in this schematic. The two optical blocks are physically connected to maintain the alignment. The dotted lines illustrate the path of scattered light collected during a scattering event.

signals provides an error check as well as the potential for estimating the refractive index of the particle similar to NCAR MASP (Baumgardner et al., 1996).

The CIP measures particle images with the same technique used by PMS 2D-OAP, i.e. capturing the shadow of the particles that pass through a focused laser (Fig. 3). A collimated laser beam from a 45-mW 0.685-μm wavelength diode laser is positioned on a

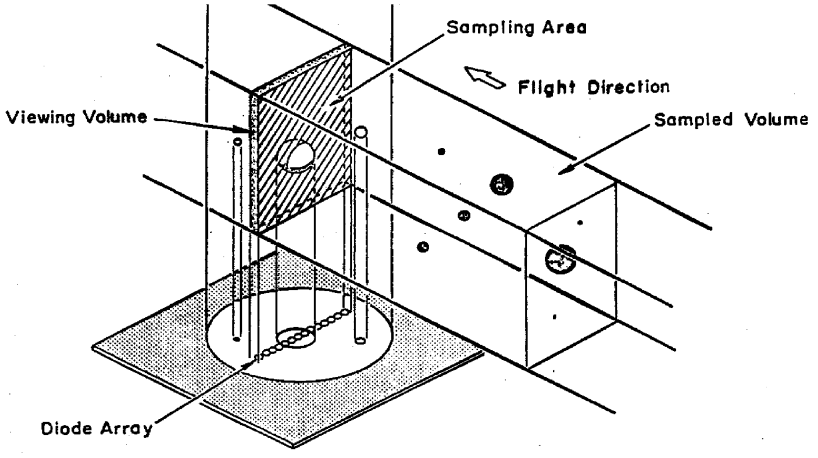

Fig. 3. The fundamental measurement principle of CIP is the imaging of the particles that pass through a collimated laser beam. Particles cast a shadow on a linear array of diodes and the processing electronics record the state of these diodes.

linear array of 64 diodes. Each time the array moves a distance of 25 μm (the probe resolution), the on–off state of each of the diodes is recorded as the particle image moves across the array. When the light level decreases by 70%, the diode state is recorded as "on." The standard PMS 2D probes use a 50% level to define the on–off state of the diodes. The 70% threshold was implemented to decrease sizing uncertainty (Korolev et al., 1998).

The LWCD uses the technique described by King et al. (1978) to measure LWC, but uses a different geometry and heat control circuit than the PMS sensor. As seen in Fig. 1, the cylindrical sensor is mounted on the edge of a rectangular strut that provides more stability and less vibration at aircraft speeds than the PMS sensor. The PMS sensor is supported between two arms and is susceptible to vibration leading to frequent breakage of the sensing element. The temperature of the wire in the DMT sensor is maintained constant by utilizing a 40-kHz signal with fixed amplitude of 28 V but with a duty cycle that varies between approximately 10% and 90%. This insures that the element is not overheated when the aircraft is at rest with no convective cooling.

The CAPS has a Pitot tube and a temperature sensor integrated in its design (Fig. 1) so that the airspeed at the location of the probe is directly measured for calculations of the sample volume and control of the CIP sampling rate.

3. Additional features and improvements

The CAPS covers the size range and capabilities of the PMS FSSP-300, FSSP-100, 2D-C and hot-wire liquid water sensor, all in a single package. Collocated measurements reduce power and space, and more importantly, provide a continuous size distribution from the same region of the cloud. The extended range of the CAS provides a continuous spectrum from aerosols in the larger end of the accumulation mode to small drizzle-sized droplets in clouds. This is an important feature when studying cloud/aerosol interactions and looking at deliquescent aerosols prior to droplet activation near the cloud base. The lower size range of the CIP has a good overlap with the upper size range measured by the CAS.

Many of the advantages of the CAPS are found in signal processing electronics. Measurements from the PMS FSSPs must be corrected for under-sizing at air speeds greater than 100 m s^{-1} caused by electronic time response limitations. The CAS with a time response of 0.1 μs does not require this correction. The FSSPs also have significant counting losses when concentrations exceed to about 500 cm^{-3} as a result of electronic dead time (Baumgardner et al., 1985; Brenguier and Amodei, 1989a,b; Brenguier et al., 1994). The CAS utilizes a first-in, first-out buffer that eliminates any dead time losses until particle rates exceed 250 K s^{-1}. At typical research airspeeds of 100 m s^{-1}, this corresponds to concentrations greater than 13,000 cm^{-3}.

Two additional features extend the capabilities of the probe for self-calibration and for evaluating the fine scale structure of aerosols and cloud particle fields. The CAS has 40 user-programmable size channels. The programmable channels allow specific sections of the Mie scattering curve to be either bracketed or selected. In the latter case, the selection of more channels in the multi-valued size range of the Mie scattering curve provides a

self-calibration as described by Brenguier et al. (1998). Shifts in where the peaks and valleys fall in the measurements within the multi-valued size region will indicate changes in the instrument due to optical misalignment, dirty optics or electronic gain changes. The second feature implemented in the CAS is the arrival time frequency distribution calculated for every time period. The frequency distribution of the time intervals between particles is an independent measure of the concentration (Baumgardner, 1986; Baumgardner et al., 1993; Brenguier et al., 1994) and also provides a measure of small-scale inhomogeneities (Paluch and Baumgardner, 1989).

The principal improvements in the CIP are added stability against vibration, larger sample volume, increased response time and decreased dead time. The 2-mW HeNe laser of the PMS OAPs has been replaced with a 45-mW diode laser. The additional intensity eliminates false triggering of the probe that has been a problem with the OAPs when vibration causes movement of the beam across the array. The CIP also has a 64-diode array for an expanded size range, and hence, a larger sample volume. The CIP can be clocked up to 8 MHz, which increases the size resolution vs. airspeed sensitivity by 60%. Conversely, for slower airspeeds, the size resolution can be increased to detect smaller particles but requires custom optics to get to the 10-μm resolution.

The electronic time response of the CIP is eight times faster than the PMS 2D probes. This eliminates the dependency of the depth of field (DOF) on airspeed (Baumgardner and Korolev, 1997). The 2D-OAPs have a particle rate limitation imposed by the amount of time required to download a particle buffer to the data system. The "overload" period, i.e. the amount of time the 2D is not taking data while downloading a buffer, is a

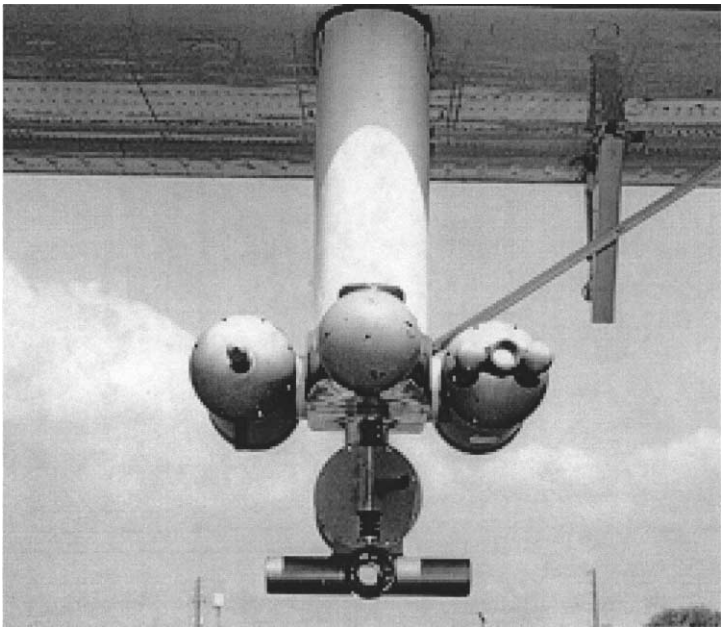

Fig. 4. The three probes compared in this paper were mounted on the same pylon of the CIRPAS Twin Otter.

function of concentration, image size and download rate. This problem has not been eliminated but has been minimized by increasing the number of images stored in a buffer by almost a factor of 10 using real-time data compression and increasing the transmission rate for downloading images by a factor of 4.

Another improvement in the CIP is the time tagging of individual particles. Each particle's arrival time in the storage buffer is the actual time of day with a resolution of 125 ns. This eliminates the decoding problem associated with PMS 2D probes where particle time is deduced from a "time word" that is actually the number of clock pulses occurring since the previous particle. These clock pulses depend upon the air speed and introduce uncertainties in the timing. In addition, each particle in the CIP buffer can be quickly decoded by reading a simple header in the buffer. This also is an improvement as

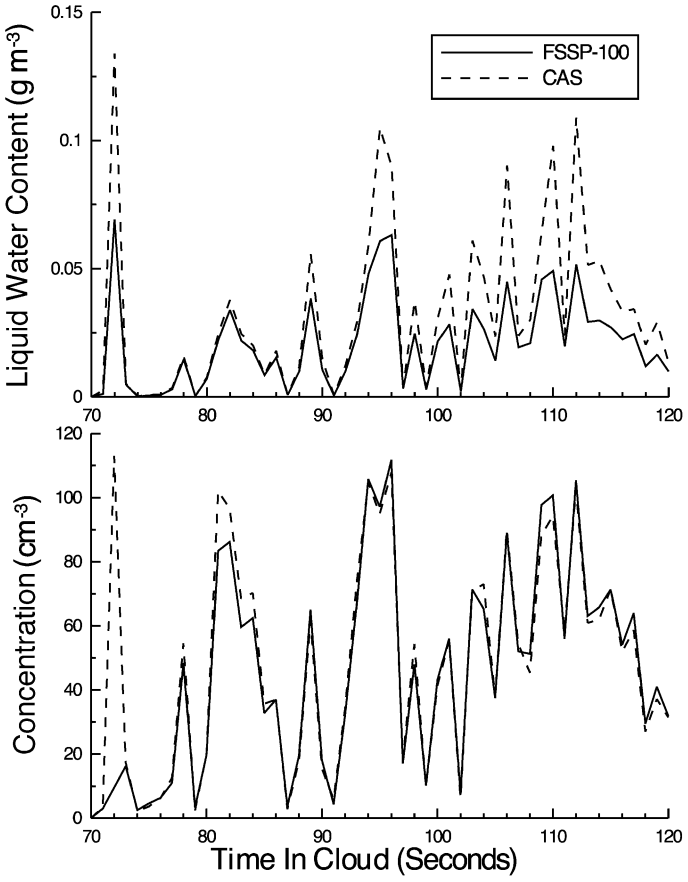

Fig. 5. LWC (top panel) and concentration (lower panel) measurements from FSSP-100 (solid line) and CAS (dashed line) are shown as a function of time in the cloud for one cloud pass during a marine stratus cloud study. The concentrations and LWCs from CAS were derived from the measurements of particles larger than 2 μm to match the lower size threshold of FSSP-100.

the PMS 2D probes use synchronization words that cannot always be easily identified and often result in missing particles.

The PMS 2D probes only store shadow images as they arrive in the sample volume. This results in an asynchronous stream of data that must be synchronized with other atmospheric parameters that are being sampled synchronously, such as state variables, water vapor, etc. The CIP measures the size of each detected particle and creates a 62-channel size distribution every second in addition to the individual image data. This is a particularly useful feature when doing calibrations prior to research flights.

The communication between the CAPS and data system is a combination of RS-232 and RS-422 high-speed serial lines. The size distribution from the CAS and CIP and the analog data from the LWC sensor, Pitot and temperature probes are sent at a baud rate of 56,000 to the RS-232 or RS-422 serial communications port on a PC or workstation.

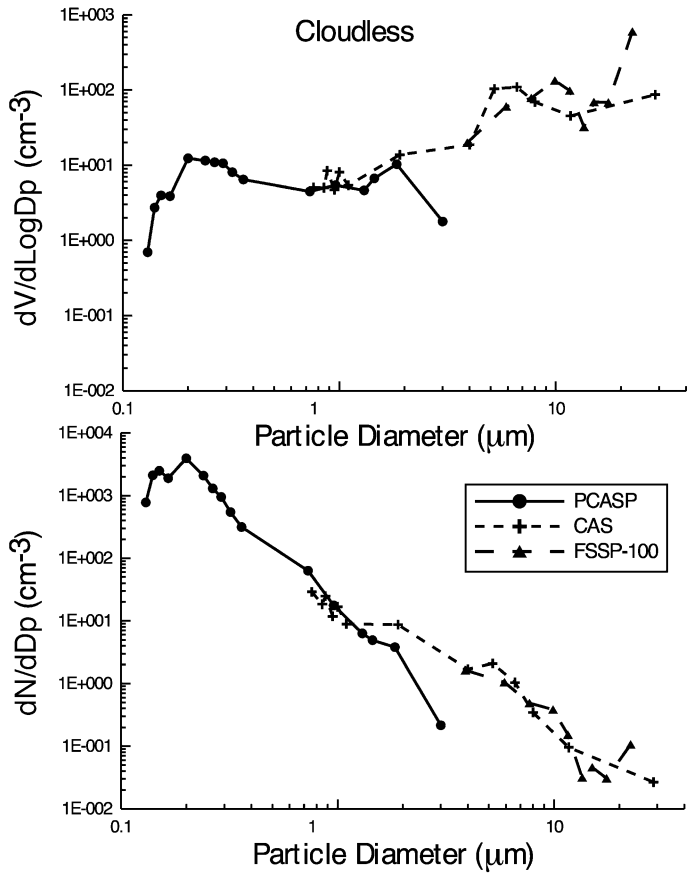

Fig. 6. The composite size distributions of concentration (top panel) and volume (lower panel) shown in this figure are constructed from a 30-min average measurement in cloudless air from PCASP (dots and solid line), CAS (crosses and dashed line) and FSSP-100 (triangle and dashed line).

Image data from the CAPS is the high-speed RS-422 sent to a commercial ISA serial interface card in the PC at 4 Mb s^{-1}.

4. Measurement examples

The CAPS was first used operationally during measurements of marine stratus near the coast of California, approximately 150 km from the Big Sur. The instrument was mounted on the Twin Otter operated by the Center for Interdisciplinary Remotely Piloted Aircraft Studies (CIRPAS). FSSP-100 and PCASP with DMT SPP electronic upgrades were also installed on this aircraft. Fig. 4 shows the respective positions of these instruments. Twenty-five flights were analyzed to compare the measurements from the particle probes and hot-wire sensor. An example of the droplet concentrations and LWCs derived from

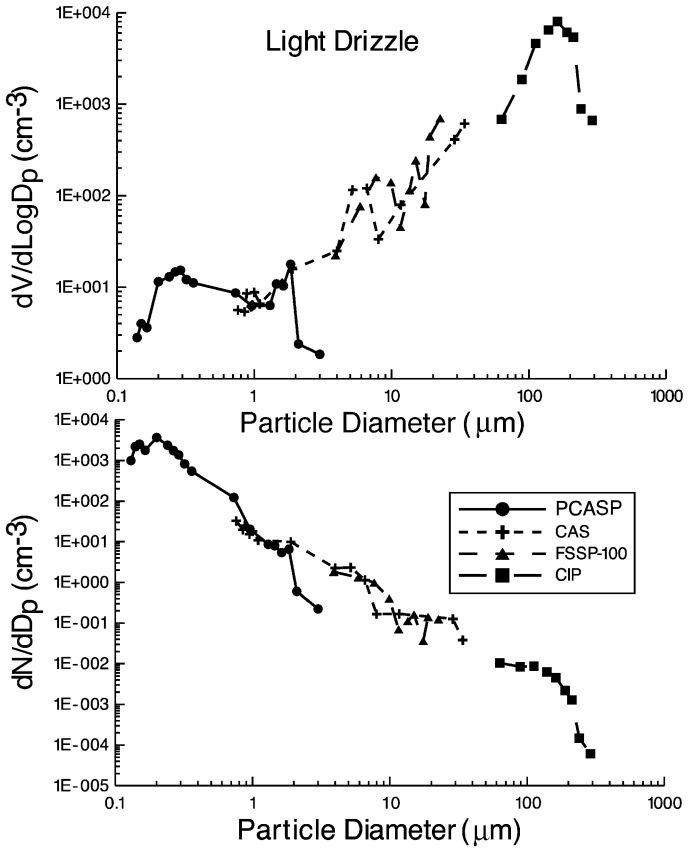

Fig. 7. The composite size distributions in this figure are from the same probes as in Fig. 6 but with the addition of CIP (boxes and dashed line) and are constructed from an average of measurements below a cloud that was producing drizzle.

FSSP-100 and CAS is shown in Fig. 5 for a single cloud pass. The FSSP-100 had been set on a nominal size range from 2 to 32 μm. The CAS measurements were analyzed over a size range from 2 to 50 μm in order to eliminate aerosol particles but highlight those areas where LWC was dominated by droplets outside the size range of FSSP-100 (>32 μm). Fig. 5 illustrates a number of interesting features when comparing the measurements from the two probes. The concentrations (lower panel) are usually in excellent agreement except in several locations where the CAS measured larger values. In those regions of higher CAS concentrations, the associated LWCs show an insignificant difference. This implies that the differences are in the smaller size categories. The likely source of these differences is in the selection of the lower size threshold used in the CAS in comparison with FSSP. We have chosen a value of 1.9 μm, the closest size to that of FSSP, but it is probable that FSSP might actually reject particles slightly larger than this size. Hence, CAS might be seeing haze droplets below the size threshold of FSSP. The LWC comparisons show that the values derived from CAS are normally larger than those from

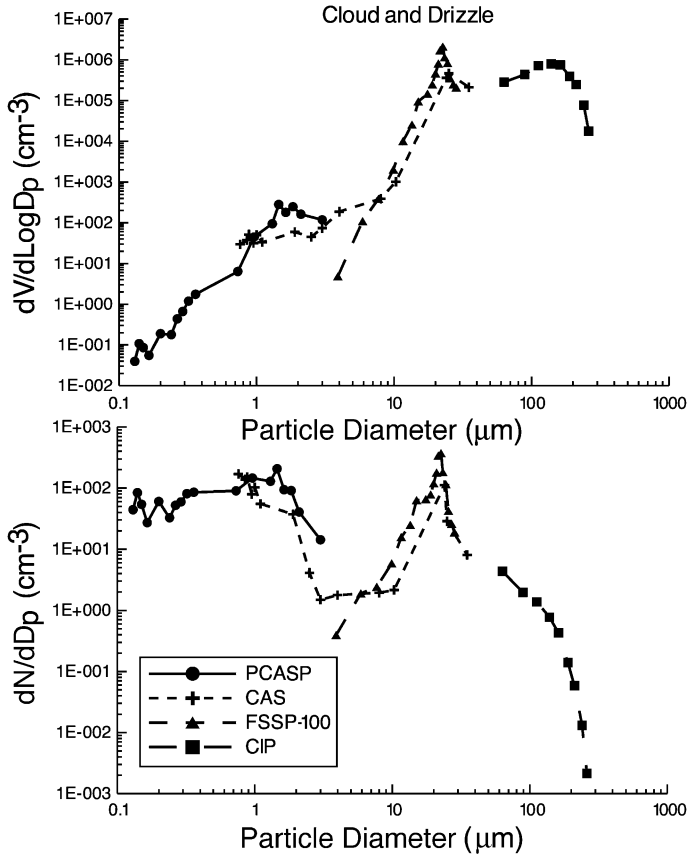

Fig. 8. The same as Fig. 9 but the measurements are averaged over a pass through a cloud that had embedded drizzle.

FSSP-100. At 72 s through the cloud, the differences can be attributed to the higher concentration measured by CAS as seen in the bottom panel. The discrepancies further into the cloud, however, are a result of the large size range of CAS since the concentrations dominated by the smaller droplets are in agreement.

Figs. 6–8 show the average concentration and volume spectra measured by the PCASP, CAS, FSSP-100 and CIP for three different environmental conditions. These comparisons demonstrate the general agreement between the different measurement systems. Fig. 8 is for cloud-free air so that the particles are only aerosols. The agreement in the overlap regions is generally good with the exception being the difference in the concentrations and volumes between PCASP and CAS at sizes larger than a micrometer. This is most likely due to the volatilization of the water in aerosols by PCASP, a

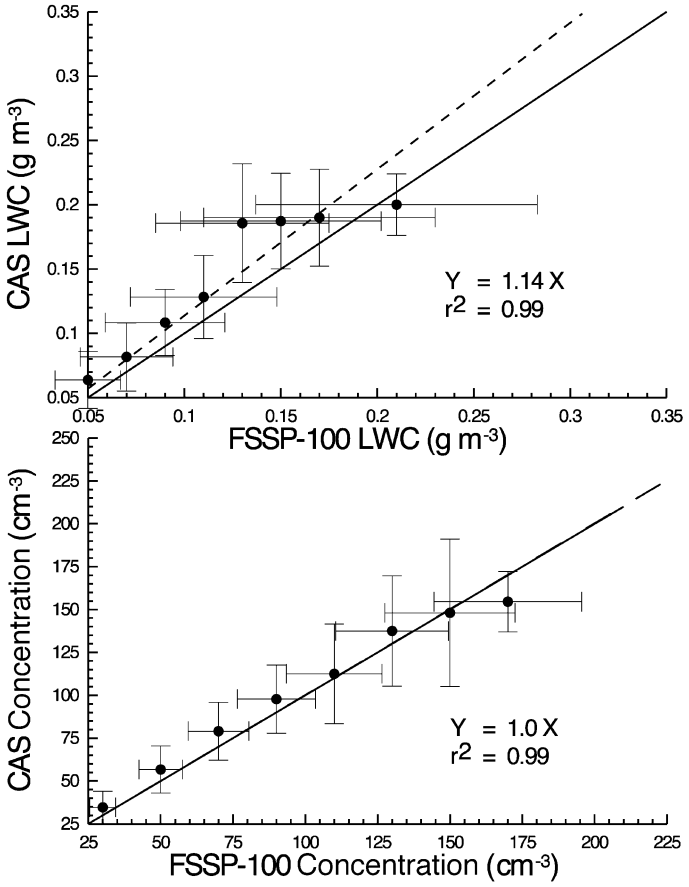

Fig. 9. The LWC (top panel) and concentration (lower panel) from FSSP-100 and CAS are the averages over 25 flights. The FSSP measurements are binned in fixed intervals over which the CAS measurements are averaged. The vertical bars at each point are the standard deviations about the average CAS values, and the horizontal bars are the estimated uncertainties for FSSP-100.

phenomenon that has been documented in other studies (Strapp et al., 1992) and results in the under-sizing by this probe. The general shape of the size spectra measured by CAS and FSSP-100 is in good agreement although the very low concentration of aerosols larger than 5 μm introduces statistical fluctuations that are to be expected.

The size distributions shown in Fig. 7 are from the measurements made in light drizzle below the clouds. This figure demonstrates the good agreement between CAS and FSSP-100 over the overlapping size range and shows that the slope of CAS matches fairly well with the slope of CIP in the small drizzle sizes.

Fig. 8 is a composite size distribution from the measurements made in a cloud with drizzle. The CAS and CIP size distributions appear to be well matched but the droplet spectrum of CAS is shifted to a larger size with respect to FSSP-100. Since the probes were calibrated with the same technique, i.e. with glass beads, this shift should not be a result of calibration differences. On the other hand, sizing corrections were not made to account for the slower response time of FSSP-100 and this might account for some of the differences. The CAS size thresholds were adjusted for a refractive index of 1.33 in this comparison, which brought the two distributions into better agreement.

Fig. 8 also shows that PCASP behaves in a different fashion than when it is in aerosols only. The concentrations of the particles larger than 1 μm exceed those measured by CAS. We can only speculate at this point that this a result of droplet shattering on the small inlet of PCASP.

The concentration and LWC measurements from CAS and FSSP-100 from all the cloud passes of 25 flights were analyzed by calculating the average CAS values for selected concentration and LWC intervals measured by FSSP-100. Fig. 9 summarizes these statistics where the horizontal bars are the estimated uncertainties in the concentration and LWC measured with FSSP-100 (Baumgardner et al., 1990), and the vertical bars at each data point are the standard deviation around the average values measured by CAS. The bottom and top panes demonstrate that the concentration and LWC measured with

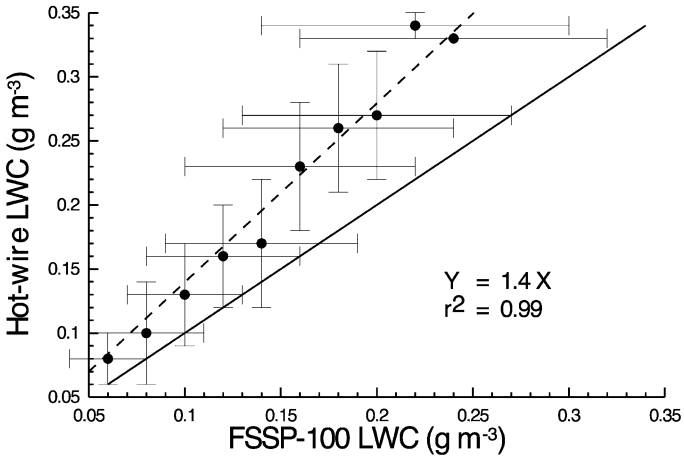

Fig. 10. The comparison between LWC from FSSP-100 and LWCD shown in this figure is for the same 25 flights used in the comparison of Fig. 9.

CAS agree with FSSP-100 within the expected uncertainties. Fig. 10 is a similar comparison between the LWCD and FSSP-100 LWCs. Both CAS and LWCD measure larger LWCs than FSSP.

5. Summary

A new aerosol, cloud and precipitation spectrometer has been developed that brings an improvement in current measurement techniques. The CAPS represents a major improvement to previous measurement techniques by using a singe system to measure a size range of particles previously requiring at least three instruments. The improved optical components and state-of-the-art electronics have eliminated or greatly minimized measurement limitations encountered with previous instruments while adding new functionality that was previously unavailable.

Acknowledgements

The authors thank Robert Bluth of the Naval Postgraduate School for his help with the development of the CAPS funded under the ONR SBIR Program, Contract No. N00014-97-C-0295.

References

Baumgardner, D., 1983. An analysis and comparison of five water droplet-measuring instruments. J. Appl. Meteorol. 22, 891–910.

Baumgardner, D., 1986. A new technique for the study of cloud microstructure. J. Atmos. Oceanic Tech. 3, 340–343.

Baumgardner, D., Korolev, A., 1997. Airspeed corrections for optical array probe sample volumes. J. Atmos. Oceanic Tech. 14, 1224–1229.

Baumgardner, D., Spowart, M., 1990. Evaluation of the forward scattering spectrometer probe: Part III. Time response and laser inhomogeneity limitations. J. Atmos. Oceanic Tech. 7, 666–672.

Baumgardner, D., Strapp, W., Dye, E., 1985. Evaluation of the forward scattering spectrometer probe: Part II. Corrections for coincidence and dead-time losses. J. Atmos. Oceanic Tech. 2, 626–632.

Baumgardner, D., Cooper, W.A., Dye, J.E., 1990. Optical and electronic limitations of the forward-scattering spectrometer probe. In: Dan Hirleman, E., Bachalo, W.D., Felton, P.G. (Eds.), Liquid Particle Size Measurement Techniques: 2nd Volume. ASTM STP, vol. 1083. American Society for Testing and Materials, Philadelphia, pp. 115–127.

Baumgardner, D., Dye, J.E., Knollenberg, R.G., Gandrud, B.W., 1992. Interpretation of measurements made by the FSSP-300X during the Airborne Arctic Stratospheric Expedition. J. Geophys. Res. 97, 8035–8046.

Baumgardner, D., Bradley, B., Kim, W., 1993. A technique for the measurement of cloud structure on centimeter scales. J. Atmos. Oceanic Tech. 10, 557–565.

Baumgardner, D., Dye, J.E., Gandrud, B., Barr, K., Kelly, K., Chan, K.R., 1996. Refractive indices of aerosols in the upper troposphere and lower stratosphere. Geophys. Res. Lett. 23, 749–752.

Brenguier, J.L., Amodei, L., 1989a. Coincidence and dead-time corrections for particle counters: Part I. A general mathematical formalism. J. Atmos. Oceanic Tech. 6, 575–584.

Brenguier, J.L., Amodei, L., 1989b. Coincidence and dead-time corrections for particles counters: Part II. High concentration measurements with an FSSP. J. Atmos. Oceanic Tech. 6, 585–598.

Brenguier, J.L., Baumgardner, D., Baker, B., 1994. A review and discussion of processing algorithms for FSSP concentration measurements. J. Atmos. Oceanic Tech. 11, 1409–1414.

Brenguier, J.L., Rodi, A.R., Gordon, G., Wechsler, P., 1998. Improvements of droplet size measurements with the fast-FSSP (Forward Scattering Spectrometer Probe). J. Atmos. Oceanic Tech. 15, 1077–1090.

Dye, J.E., Baumgardner, D., 1984. Evaluation of the forward-scattering spectrometer probe: I. Electronic and optical studies. J. Atmos. Oceanic Tech. 1, 329–344.

King, W.D., Parkin, D.A., Handsworth, R.J., 1978. A hot wire water device having fully calculable response characteristics. J. Appl. Meteorol. 17, 1809–1813.

Knollenberg, R.G., 1981. Techniques for probing cloud microstructure. In: Hobbs, P.V., Deepak, A. (Eds.), Clouds, Their Formation, Optical Properties and Effects. Academic Press, New York, pp. 15–92.

Korolev, A.V., Kuznetsov, S.V., Makarov, Yu E., Nonikov, V.S., 1991. Evaluation of measurements of particle size and sample area from optical array probes. J. Atmos. Oceanic Tech. 8, 514–522.

Korolev, A.V., Strapp, J.W., Isaac, G.A., 1998. Evaluation of the accuracy of PMS optical array probes. J. Atmos. Oceanic Tech. 15, 708–720.

Paluch, I.R., Baumgardener, D.G., 1989. Entrainment and fine-scale mixing in continental convective clouds. J. Atmos. Sci. 46, 261–278.

Strapp, J.W., Leaitch, W.R., Liu, P.S.K., 1992. Hydrated and dried aerosol-size-distribution measurements from the Particle Measuring Systems FSSP-300 probe and the deiced PCASP-100X probe. J. Atmos. Oceanic Tech. 9, 548–555.

Wendisch, M., Keil, A., Korolev, A.V., 1996. FSSP characterization with monodispersed water droplets. J. Atmos. Oceanic Tech. 13, 1152–1165.